Extended Abstracts of the 2016 International Conference on Solid State Devices and Materials, Tsukuba, 2016, pp69-70

B-1-04

Switching Mechanism in Resistive Random Access Memory by First-Principles Calculation Using Practical Model Based on Experimental Results

Takumi Moriyama[1], Takahiro Yamasaki[2], Sohta Hida[1], Takahisa Ohno[2,3], Satoru Kishida[1,4] and Kentaro Kinoshita[1,4]

[1] Tottori University, 4-101 Koyama-Minami, Tottori 680-8552, Japan.
[2]Natonal Institute for Materials Science (NIMS), Namiki 1-1, Tsukuba, Ibaraki 305-0044, Japan.
[3]Institute of Industrial Science, the University of Tokyo, 4-6-1 Komaba, Meguro-ku, Tokyo 153-8505, Japan.
[4]Tottori Integrated Frontier Research Center (TiFREC), 4-101 Koyama-Minami, Tottori 680-8552, Japan
Phone: +81-857-31-5244, E-mail: kinoshita@ele.tottori-u.ac.jp

Abstract

This paper reports on resistive switching (RS) mechanisms of a Pt/polycrystalline NiO/Pt-ReRAM structure by using both experiments and first-principles calculations. We constructed a grain model based on our experimental data, and allocated surface orientations of the grain based upon calculated surface energies. We found that the width of band gap depends on the surface orientation, and that conductive surface can become insulating easily with slight displacement of surface atoms, which explains the RS mechanism.

1. Introduction

For practical use of Resistive Random Access Memory (ReRAM), understanding the resistive switching (RS) mechanism in transition metal oxides (TMO) is important. Some papers predict its mechanism by using first-principles calculation; for example, TMO become conductive by introducing oxygen vacancies in bulk single crystalline TMO [1]. However, it is reported that the RS were caused in the domain-boundaries of single crystalline TMO [2] and the RS were caused in the grain boundaries of polycrystalline TMO [3]. In this study, we constructed a grain model based on our experimental data and suggested where conductive path exists in polycrystalline NiO films.

2. Experimental and theoretical methods.

A Pt top electrode was deposited on NiO(60 nm)/Pt(100 nm) structure by sputtering method, and the contact area of the sputtered electrode is ϕ100 μm. This structure will be referred to as a sputtering deposited electrode (SD-EL) sample hereafter. To compare the properties of RS, we also used a soft-probe [4] with which we can form an electric contact without physically damaging the surface of samples. By contacting the Pt soft-probe to the surface of the NiO/Pt film, a Pt/NiO/Pt sturucture is formed in the contact area. The effective contact area of the Pt soft-probe, where a Pt/NiO/Pt structure is formed, was estimated to ϕ100 μm. This structure will be referred to as a soft-probe contact electrode (SC-EL) sample. We measured current-voltage (*I*-*V*) characteristics of SD- and SD-EL samples, and extracted the set voltage, V_{set}, and reset voltage, V_{reset}.

We used a first-principles calculation program PHASE/0[5] based on DFT to decide appropriate surface orientations of experimentally observed NiO grains and to analyze the electronic states of the surfaces. We used the GGA+U [6] and set U_{eff} = 5.3 eV. Repeated slab models were used to calculate surface energies, E_{surf}'s, and electronic states of various orientations.

3. Results and Discussion

Figures 1(a) and (b) respectively show the surface and cross-sectional images of SEM of the NiO/Pt structure. We can find that NiO film has a polycrystalline structure and consists of columnar crystal grains on each of which a trigonal pyramid caps. A XRD pattern exhibited a (111) preferred orientation of rock-salt type structure for the NiO film. Based on these experimental data, we postulated a triangular prism structure with a trigonal pyramid on it as the grain model as shown in Fig. 1(c). We allocate (100), (010) and (001) to the surfaces of the trigonal pyramids, and (-211), (1-21) and (11-2) to the surfaces of trigonal prisms based upon calculcated E_{surf}'s. Here, we assumed that each of grain boundaries of polycryctalline NiO films is consisted of oppositely facing two surfaces of single crystals separated with a gap space.

Figures 2(a) and (b) show LDOS's of Ni and O atoms on the (001) and (11-2) surfaces, respectively. The (001) surface has a band gap of 2.6 eV, while the (11-2) surface has no band gap. This suggests that the (11-2) surface has higher conductivity than the (001) surface and electric current flows through the side surfaces of the grain (i.e., the grain boundaries). This calculation result agrees with the experimental result: SEM images and electron beam absorption current images suggest that the grain boundaries have higher conductance than inside of the grains.

Figure 3(a) shows *I*-*V* characteristics of forming of SD- and SC-EL samples. Forming voltages of SC-EL samples are higher than those of SD-EL samples. Figs. 3(b) and (c) show the cumulative probabilities of V_{set} and V_{reset}, respectively. V_{set}'s and V_{reset}'s of SC-EL samples are close to respective values of SD-EL samples at the low voltage area. These phenomena can be explained with an additional assumption of the grain model: the side surfaces of the grain model consist not only of conductive (11-2) surfaces but also of insulating surfaces, and total conductivities of the side surfaces of the grain are ruled by the rates of conductive (11-2) surfaces and insulating surfaces (a schematic view put at lower place in Fig. 4(a)). Figures 4(b) and (c)

show the cross-sectional schematics of the SD- and SC-EL samples, respectively. Conductivities of SD-EL samples strongly depend on surface conductivities of the side surfaces of the grain and RS causes on the insulating surfaces at the side surfaces of the grain because the deposited Pt contacts to the rough polycrystalline NiO surface with no spaces as shown in Fig. 4(b). For SC-EL samples, on the other hand, the Pt soft-probe contact only on tops of the triangular prisms as shown in Fig. 4(c). For the RS, the surfaces of the triangular prism, which is insulating (001) surface, have to become conductive, accordingly forming voltages of SC-EL samples are higher than those of SD-EL samples.

Considering the calculation results of LDOS on (001) and (11-2) surfaces shown in Figs. 2(a) and (b), we propose a mechanism of RS. Figures. 5(a) and (b) show the schematics of the side surfaces of the grains for a low and a high resistance state, respectively. Whereas the surface of the low resistance state is the conductive (11-2) surface (Fig. 5(a)), the surface of the high resistance state has narrow (001) terraces on the (11-2) surface (Fig. 5(b)). The structural change between Figs. 5(a) and (b) can be caused by slightly displacing pairs of neighboring nickel and oxygen atoms. The widths of band gap of the high resistance surface shown in Fig. 5(b) is 1.1 eV.

4. Conclusions

To elucidate the mechanism of RS of a Pt/ polycrystalline NiO/Pt-ReRAM, we constructed a grain model of NiO based on our experimental data and allocated appropriate orientations to the surfaces of the grain through calculated stabilities of various surfaces. Structure-dependences of *I-V* characteristics indicate that the conductive switching paths are formed on the side surfaces of the grains (i.e., in grain boundaries), whereas the allocated ideal (11-2) surface of the grain is conductive. We found that a (001) terrace structure introduced to the (11-2) surface by slight displacements of small amount of atoms changes the surface conductivity drastically, which explains the experimental phenomena.

Acknowledgement

Pt soft-probes were supplied by Dr. M. Yoshitake from NIMS. The numerical calculations were carried out by using the supercomputers of the Institute for Solid State Physics at Tokyo Univ., Institute for Information Management and Communication at Kyoto Univ., and Numerical Materials Simulator at NIMS.

References

[1] H. D. Lee *et al.*, Phys. Rev. B **81**, 193202 (2010).
[2] M. Kawai *et al.*, Appl. Phys. Lett. **95**, 012109 (2009).
[3] G.-S. Park *et al.*, Appl. Phys. Lett. **91**, 222103 (2007).
[4] M. Yoshitake *et al.*, e-J. Surf. Sci. Nanotech. **13**, 307 (2015).
[5] https://azuma.nims.go.jp/
[6] J. P. Perdew *et al.*, Phys. Rev. Lett. **77**, 3865 (1996).

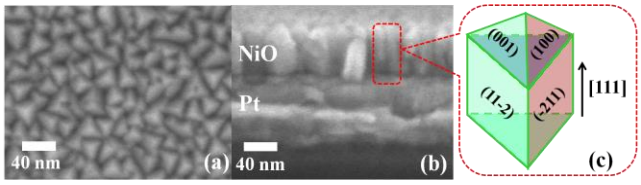

Fig. 1 (a) Surface and (b) cross-sectional SEM images of a NiO/Pt structure. (c) NiO grain model based on the surface and cross-sectional SEM images of NiO.

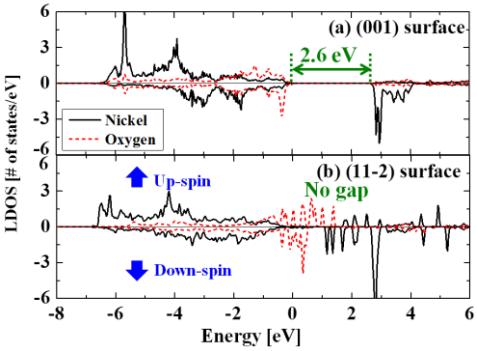

Fig. 2 LDOS's of a nickel (dashed) and an oxygen (broken) atom on (a) the (001) and (b) the (11-2) surface.

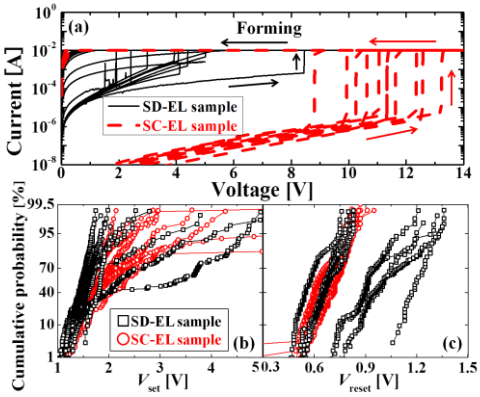

Fig. 3 (a) *I-V* characteristics of forming, and cumulative probabilities of (b) V_{set} and (c) V_{reset} of SD- and SC-EL samples.

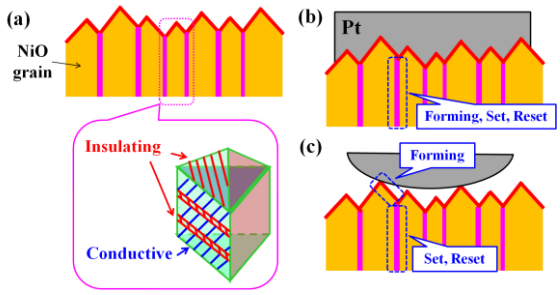

Fig. 4 (a) The grain models which consist of conductive surface and insulating surface, and the cross-sectional schematics of (b) the SD- and (c) the SC-EL samples.

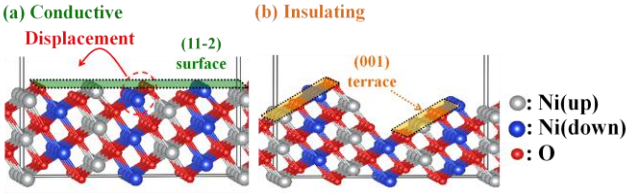

Fig. 5 Schematics of the side surface of the grain for (a) a low and (b) a high resistance state.